JOURNAL OF GEOPHYSICAL RESEARCH, VOL. 90, NO. C1, PAGES 1061–1067, JANUARY 20, 1985

Removal of Ambiguity of Two-Dimensional Power Spectra Obtained by Processing Ship Radar Images of Ocean Waves

V. ATANASSOV,[1] W. ROSENTHAL, AND F. ZIEMER[2]

Institut für Meereskunde der Universität Hamburg and Max-Planck-Institut für Meteorologie, Hamburg

The usual spatial power spectra of ocean wave images taken from PPI of a ship radar show an ambiguity in the wave propagation direction. A simple numerical procedure is suggested and realized to remove this ambiguity. It makes use of the data from two consecutive turns of the radar antenna as well as of the wave dispersion law. The results obtained show a good agreement with the ground truth.

1. INTRODUCTION

The attention of many oceanographers has been attracted by the use of coastal/shipborne microwave imaging radars in ocean wave studies [*Mattie and Harris*, 1978]. Recently, it has been proposed that digitized pictures of ship radar images of ocean waves be processed in order to obtain the spectral characteristics of the surface wave field. The corresponding scheme (backscattered microwave power → light intensity of the radar screen → gray level density on a film → numerical gray level → two-dimensional Fourier transform) is considered by *Hoogeboom and Rosenthal* [1982]. The imaging takes place owing to the modulation of the backscattered microwave power by the long ocean waves through short-wavelength Bragg-scattering waves as well as effects of shadowing by the wave crests (important at low grazing angles). The preliminary studies [*Ziemer and Rosenthal*, 1983] show by calculating two-dimensional power spectra that the spectral properties of such images are similar to those obtained from the conventional pitch-and-roll buoy measurements. The spectral value of each wave number seems to be a well-defined function of the corresponding value of the directional surface wave spectrum, depending smoothly on the environmental and radar parameters.

Hence two-dimensional power spectra obtained by processing ship radar images contain useful information about the wave directionality. However, owing to the point symmetry of the spatial power spectrum, it is not possible to distinguish the area of the actual wave train and its dual image in the wave number plane. In particular, uncertainty of 180° (ambiguity) remains in the determination of the wave propagation direction. It is hardly possible to remove this ambiguity simply looking at the image of an irregular wave field. This disadvantage is usually overcome by assuming that waves travel inshore [*Mattie et al.*, 1981] or downwind, which requires additional information and leaves aside the possible detection of upwind traveling waves [cf. *Braun*, 1982], wave reflection from obstacles [*Wadhams*, 1978], or backscatter caused by bottom irregularities [*Long*, 1973]. In the last two cases the power spectra of the main and reflected wave trains usually occupy the same region of the wave number plane and hence remain undistinguishable.

In this study we suggest a possible solution of the ambiguity problem for spatial power spectra of arbitrary wave fields by processing two images in the spectral domain, the second obtained shortly after the first one, making use of the known dispersion relation. The corresponding numerical procedure is applied for artificially created pairs of wave images as well as to processing radar screen images of a real sea surface. In the latter case a comparison with pitch-and-roll buoy data has been made.

Since the ambiguity problem arises for any momentary spatial wave field measurements, we hope that the method considered here could apply also for data processing in other imaging systems as side-looking airborne radar (SLAR) [cf. *McLeish and Ross*, 1983], synthetic aperature radar (SAR) [cf. *McLeish et al.*, 1980; *Alpers et al.*, 1981], or stereophotography [*Holthuijsen*, 1983].

2. THE PHYSICAL PICTURE AND BASIC ASSUMPTIONS

Surface waves in the field are usually treated in a statistical sense. The sea state at one location for given environmental parameters (e.g., wind speed, bottom topography, etc.) is described by the statistical ensemble of surface wave fields possible for these parameters. Each member of the ensemble behaves, of course, according to the deterministic equations of motion.

In this paper we study the wave field over a selected quadratic area with a side length of about 650 m in a deterministic manner. We assume that the wave field develops in time according to the linearized equations of motion such that a linear superposition of sine waves is adequate for the mathematical description. We emphasize that statistical quantities of sea state description such as decorrelation length are meaningless in this deterministic picture. After the ambiguity in the two-dimensional spectrum is removed, it may serve, of course, as an estimator of the spectral expectation values for the prescribed environmental conditions. Each wave number then exhibits 2 degrees of freedom. It may be argued that the inclusion of two images for processing produces 4 degrees of freedom. However, the two successive images being used for one unambiguous spectrum are the same deterministic realization of the statistical ensemble that defines the sea state for the prescribed environmental conditions. The number of degrees of freedom can be increased as usual by averaging over independent samples.

Instead of the surface waves itself we study the time development of their images on the radar screen. For the proposed method we have to assume that there is a linear relationship between the single sinusoidal wave component and its image

[1] On leave from Institute of Electronics, Sofia, Bulgaria.
[2] Also at Deutsches Hydrographisches Institut, Hamburg.

Paper number 4C1094.
0148-0227/85/004C-1094$05.00

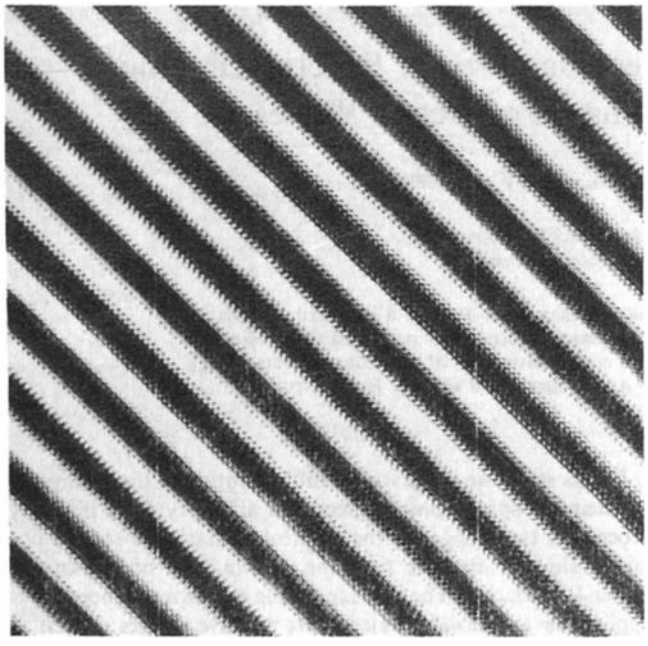

Fig. 1*a*

Fig. 1. (*a*) Gray scale image of a single sin wave and its two-dimensional power spectra (*b*) with and (*c*) without ambiguity. The isolines represent relative intensity increasing in steps of 4^k ($k = 0, 1, 2, 3, 4$) counted from the periphery of the wave number plane. Here and further on we omit the time-delayed second image and its power spectrum.

on the radar screen. Especially the space-time behavior of a single wave component that may be described by exp ($i\mathbf{k} \cdot \mathbf{x} - i\omega t$) must be reproduced by the image. This property has been checked by comparing the theoretical and measured phase increment ωt between successive images for single Fourier components with fixed wave number $\mathbf{k}$. From the successful suppression of the ambiguous part of the wave spectrum shown in section 4, it may be deduced a posteriori that the Fourier components of the wave field and the corresponding Fourier components on the radar screen indeed show the same time dependence.

3. Theoretical Background and Simulation

Consider a wave train:

$$\zeta(\mathbf{r}, t) = (2\pi)^{-2} \int d\mathbf{k} a(\mathbf{k}) \cos [\mathbf{k} \cdot \mathbf{r} - \omega(\mathbf{k})t + \phi(\mathbf{k})]$$

$$= (2\pi)^{-2} Re \int d\mathbf{k} \eta(\mathbf{k}) \exp [-i\omega(\mathbf{k})t + i\mathbf{k} \cdot \mathbf{r}] \quad (1)$$

where $\zeta(\mathbf{r}, t)$ represents a two-dimensional data field depending on time, $\eta(\mathbf{k}) = a(\mathbf{k}) \exp [i\phi(\mathbf{k})]$ is the true complex amplitude of the wave packet and $\omega(\mathbf{k}) = 2\pi f(\mathbf{k})$ is then positive wave frequency, obtained from the known dispersion relation; the rest of notation is standard. The spatial Fourier transform of (1) is

$$\zeta(\mathbf{k}, t) = \int d\mathbf{r} \zeta(\mathbf{r}, t) \exp (-i\mathbf{k} \cdot \mathbf{r})$$

$$= \tfrac{1}{2}\{\eta(\mathbf{k}) \exp [-i\omega(\mathbf{k})t] + \eta^*(-\mathbf{k}) \exp [i\omega(-\mathbf{k})t]\} \quad (2)$$

Thus we see that a duality appears in the corresponding power spectrum:

$$|\zeta(\mathbf{k}, t)|^2 = |\zeta(-\mathbf{k}, t)|^2$$

$$= \tfrac{1}{4}\{|\eta(\mathbf{k})|^2 + |\eta(-\mathbf{k})|^2 + 2\, Re\, [\eta(\mathbf{k})\eta(-\mathbf{k}) \exp [-i(\omega(\mathbf{k}) + \omega(-\mathbf{k}))t]]\} \quad (3)$$

However, by knowing $\zeta(\mathbf{k}, t)$ in two consecutive moments t_1 and $t_2 = t_1 + \tau$, one may calculate

$$\Delta_+(\mathbf{k}) = 2\{1 - \cos [\omega(\mathbf{k}) + \omega(-\mathbf{k})]\tau\}^{-1} \cdot \{|\zeta(\mathbf{k}, t_1)|^2 + |\zeta(\mathbf{k}, t_2)|^2 - 2\, Re\, [\zeta(\mathbf{k}, t_1)\zeta^*(\mathbf{k}, t_2) \exp (i\omega(-\mathbf{k})\tau)]\} \quad (4)$$

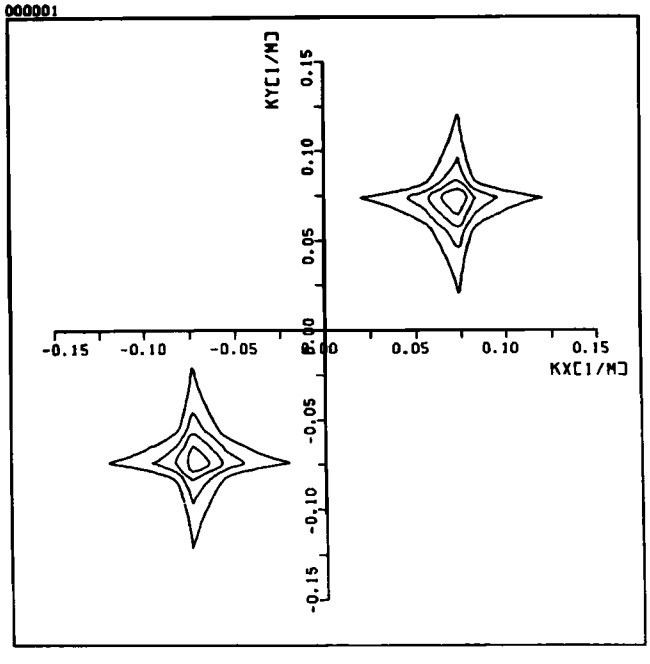

Fig. 1*b*

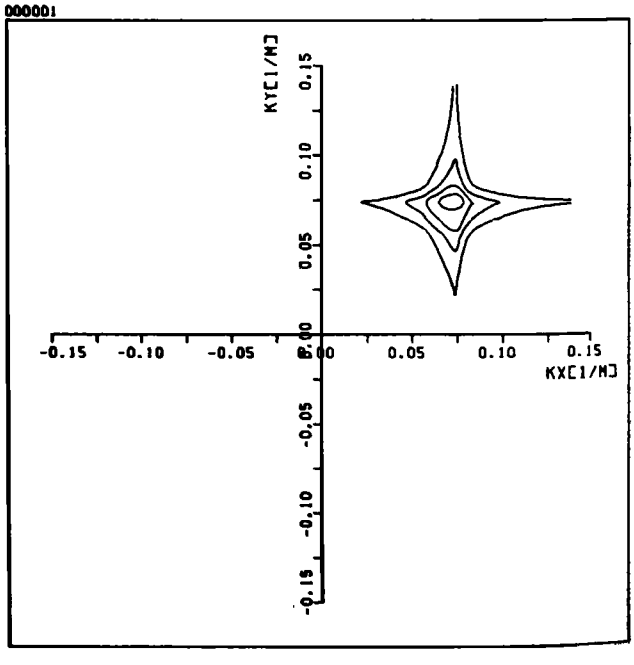

Fig. 1*c*

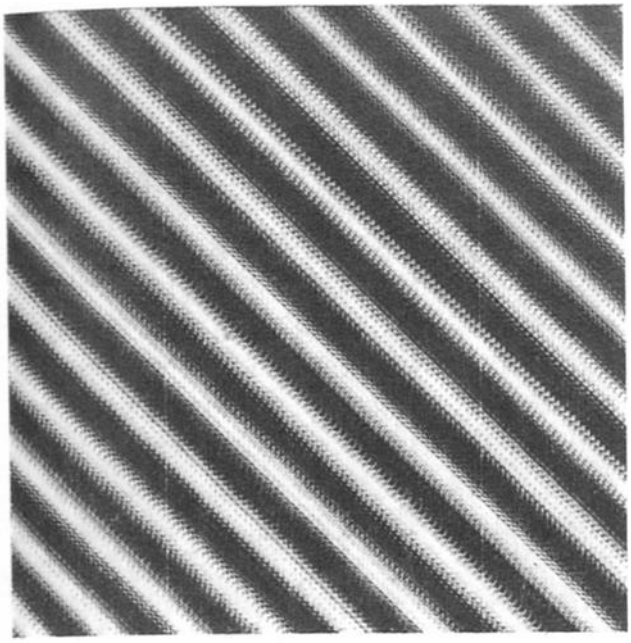

Fig. 2a

Fig. 2. (*a*) Gray scale image of two sin waves, simulating wave reflection and the corresponding two-dimensional power spectra (*b*) with and (*c*) without ambiguity. The isolines are as described in Figure 1.

and

$$\Delta_-(\mathbf{k}) = 2\{1 - \cos[\omega(\mathbf{k}) + \omega(-\mathbf{k})]\tau\}^{-1} \cdot \{|\zeta(\mathbf{k}, t_1)|^2 + |\zeta(\mathbf{k}, t_2)|^2 - 2\,Re\,[\zeta(\mathbf{k}, t_1)\zeta^*(\mathbf{k}, t_2)\exp(-i\omega(\mathbf{k})\tau)]\} \quad (5)$$

thus separating the actual power spectrum $\Delta_+(\mathbf{k}) = |\eta(\mathbf{k})|^2$ from its dual image $\Delta_-(\mathbf{k}) = |\eta(-\mathbf{k})|^2$. The time delay determines the frequency and wave number range of the surface wave field that can be treated, because of the restriction

$$0 < [\omega(\mathbf{k}) + \omega(-\mathbf{k})]\tau < 2\pi \quad (6)$$

It should be noted that

$$\omega(\mathbf{k}) > 0 \quad (7)$$

must be satisfied. For a symmetric wave dispersion relation $\omega(\mathbf{k}) = \omega(-\mathbf{k})$, (6) includes (7) and implies that the upper limit of the frequency spectrum interval equals Nyquist frequency for a sampling period τ:

$$0 < f(\mathbf{k}) < 1/2\tau \quad (8)$$

Therefore it should be kept in mind that separation takes place in certain area of the wave number space where (6) and (7), or in particular (8), are fulfilled. For a deep-water gravity surface wave dispersion law $\omega(k) = (gk)^{1/2}$ the method is good provided that

$$0 < k < \pi^2/g\tau^2 \quad (9)$$

The time delay τ usually equals the antenna rotation period. For time delay of 2.2 s, used throughout in this study, it seems to be possible to separate wave trains with frequency less than 0.23 Hz and wavelengths longer than 30 m, as obtained from (9). These restrictions are not so severe, bearing in mind that the spatial resolution of the commercially available ship radars in radial direction is about 10 m.

A FORTRAN program realizing (4) has been constructed and checked with pairs of artificially created digital monochromatic wave images. Each image is stored in a 128 × 128 pixel matrix which corresponds to area of 676 × 676 m^2 and gives spectral resolution of 9.2×10^{-3} m^{-1}. These values have been chosen to coincide with those of the real sea surface ship radar images considered in section 4. The linear gravity surface wave dispersion relation for finite depth H:

$$\omega(k) = (gk \tanh kH)^{1/2} \quad (10)$$

has been used, but Doppler shift corrections can also be included.

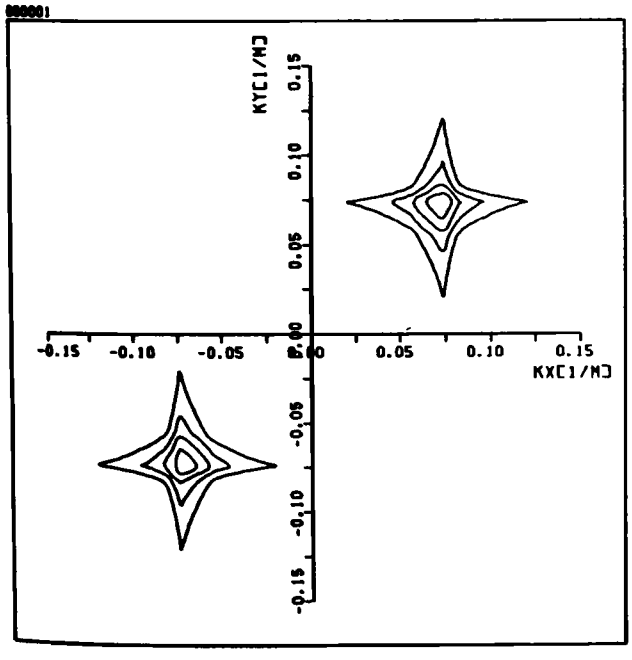

Fig. 2b

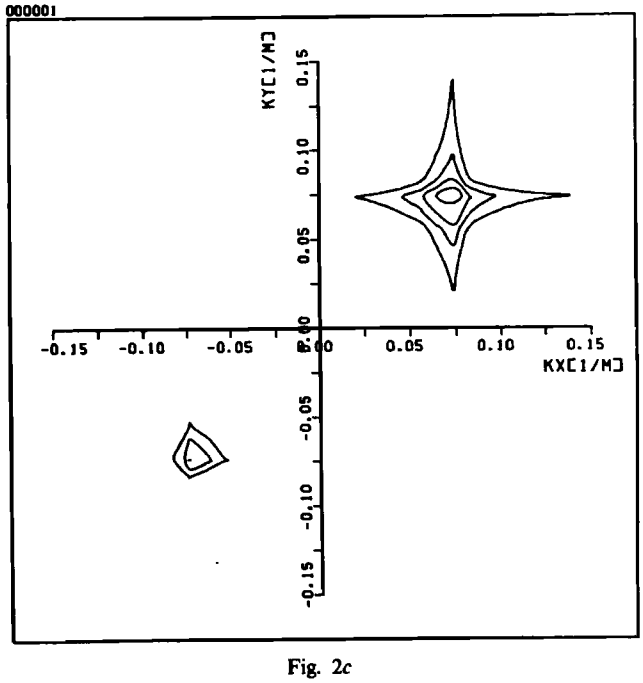

Fig. 2c

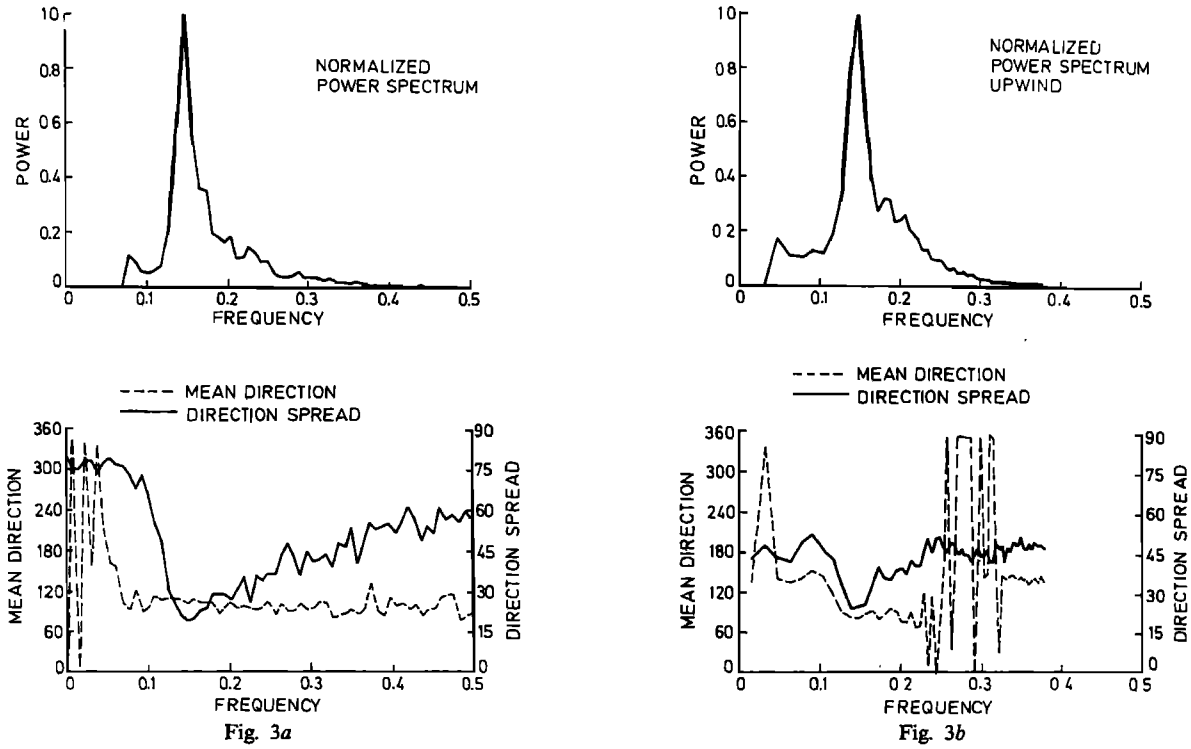

Fig. 3a Fig. 3b

Fig. 3. (*a*) Pitch-and-roll buoy and (*b*) radar-obtained frequency spectra, mean direction, and angular spread in the case of wind waves (case I).

The numerical gray level has been taken in the form

$$A(x_m, y_n, t) = \sum_{i=1}^{2} A_i\{1 + \cos [k_0(x_m \cos \alpha_i + y_n \sin \alpha_i) - \omega(k_0)t + \phi_i]\} \quad (11)$$

where $x_m = (m-1)L/(N-1)$, $y_n = (n-1)L/(N-1)$ for $m, n = 1, 2, \cdots, N$; with $N = 128$ and $L = 676$ m; A_i and α_i are the amplitudes and propagation angles of the waves in the image.

The ability of the procedure to remove the two-dimensional spatial power spectra ambiguity is clearly illustrated by Figure 1, which presents the results in the simplest case of one monochromatic wave ($A_1 = 128$, $\alpha_1 = \pi/4$; $A_2 = 0$) with wavelength of 63 m ($k_0 = 0.10$ m^{-1}) and frequency f of 0.157 Hz derived from (10) for $H = 30$ m. Figure 2 ($A_1 = 80$, $\alpha_1 = \pi/4$; $A_2 = 40$, $\alpha_2 = 5\pi/4$) demonstrates the separation of wave trains traveling in opposite directions. The existence of the second wave cannot be deduced either by looking at the images or at the plots of the power specctra calculated by using (3). The advantage of (4) may be useful, in particular, for detecting waves reflected from obstacles [*Wadhams*, 1978] or, possibly, upwind waves. It is worth noting that the ratio of the peak maxima may give a good estimate of the reflection constant $R = A_2^2/A_1^2$.

Errors in wave parameters derived by radar are discussed by *Mattie and Harris* [1978] in the image domain. They can easily be transferred to the spectral domain used in this paper. Let us therefore only consider the influence of systematic or random errors on the calculated unambiguous spectrum $\Delta_+(\mathbf{k})$. Since both phase and amplitude relations are used in (4), we can classify the errors as phase and amplitude ones and consider them separately.

The first group appear first of all due to inaccuracy of the dispersion relation used in (4), i.e., the "actual" unknown dispersion law $\tilde{\omega}(\mathbf{k})$ may differ from the theoretical one (10) for several reasons as Doppler shift due to currents or ship motion, nonlinear dispersion, or frequency spread. This situation arises even in the simulations (Figures 1–2) because of the broadening in wave number space due to the finite size of the images. The resulting spectrum is the convolution of the original delta-peaked spectrum and the Fourier transform of the spatial window. Since this window has no time dependence, the resulting smeared spectrum has to be analyzed by (4) with the central frequency $\omega(k_0)$ for all wave numbers. Phase errors may also appear due to improper positioning of the pictures (geometrical displacement of the second radar screen image with respect to the first one). We denote the actual unknown complex wave amplitude with $\tilde{\eta}(\mathbf{k})$ and assume that for any wave number $\mathbf{k}$ with non-vanishing amplitude $\tilde{\eta}(\mathbf{k})$, the corresponding $\tilde{\eta}(-\mathbf{k}) = 0$, i.e., no symmetry initially occurs. We arrive at

$$\Delta_+(\mathbf{k}) - |\tilde{\eta}(\mathbf{k})|^2 = 2\{1 - \cos [\omega(\mathbf{k}) + \omega(-\mathbf{k})]\tau\}^{-1} \cdot \{|\tilde{\eta}(\mathbf{k})|^2 \sin \tfrac{1}{2}\delta(\mathbf{k}) \sin [\tfrac{1}{2}\delta(\mathbf{k}) - (\omega(\mathbf{k}) + \omega(-\mathbf{k}))\tau] + |\tilde{\eta}(-\mathbf{k})|^2 \sin \tfrac{1}{2}\delta(\mathbf{k})\} \quad (12)$$

where

$$\delta(\mathbf{k}) = [\omega(\mathbf{k}) - \tilde{\omega}(\mathbf{k})]\tau + \mathbf{k} \cdot \mathbf{r}_0$$

gives the total phase error due to dispersion inaccuracy and geometrical displacement $\mathbf{r}_0$ (projected on the sea surface) of the second image with respect to the first one.

The amplitude errors may appear for instance due to systematic variation of the screen intensity or variation of the camera shutter speed. For the simple case of a multiplicative

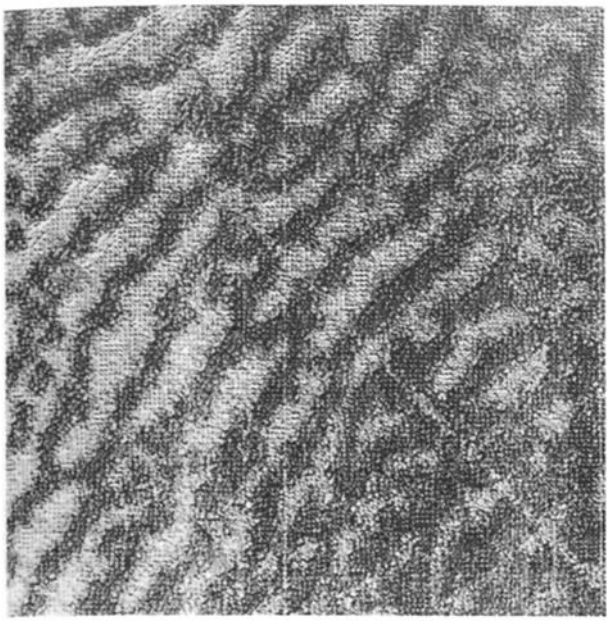

Fig. 4*a*

Fig. 4. (*a*) Gray scale radar PPI image and its two-dimensional power spectra (*b*) with and (*c*) without ambiguity in the case of wind waves. The isolines represent relative intensity of 2^k ($k = 0, 1, 2$) counted from the periphery of the wave number plane.

error $(1 + \varepsilon)$ in the second image, we obtain

$$\Delta_+(\mathbf{k}) - |\tilde{\eta}(\mathbf{k})|^2 = \varepsilon|\tilde{\eta}(\mathbf{k})|^2 + \tfrac{1}{2}\varepsilon^2[|\tilde{\eta}(\mathbf{k})|^2 + |\tilde{\eta}(-\mathbf{k})|^2] \cdot \{1 - \cos[\omega(\mathbf{k}) + \omega(-\mathbf{k})]\tau\}^{-1} \quad (13)$$

We can conclude that the phase and amplitude errors are considerably enhanced in the vicinity of wave numbers satisfying $[\omega(\mathbf{k}) + \omega(-\mathbf{k})] = 2\pi$.

4. Processing of Ship Radar Images of a Real Sea Surface

The numerical procedure suggested in the previous chapter has been applied to process digitized images of sea surface on a ship radar PPI in natural conditions. The data have been collected during cruises of the DHI research ship *Gauss* near the research platform "Nordsee" as well as west from the North Sea island Sylt.

An X-band Raytheon (Ray TM/EP1650/9XR) radar has been used, with parameters described as follows: nominal peak power of 50 kW, pulse width of 60 ns at 0.75–3 mi range, PRF of 3600 s^{-1}, antenna rotation speed of 27 rpm, HH polarization and horizontal/vertical beamwidth (at 3 dB) of 0.85°/22°. The pictures have been taken by means of a motor driven 24 × 36 mm camera. We emphasize that proper positioning of both images in the gray level matrix up to a pixel has been achieved during the digitizing procedure.

From various successful tests we have chosen two cases to demonstrate the method. The first event is an almost ideal growing wind sea if we consider the one-dimensional spectrum, the mean direction, and the directional spread as measured by a pitch-and-roll buoy (Figure 3*a*). The wind was rather steady, with a speed of 9.7 m/s and direction from 267°. The ship was anchored and heading to 293°. The significant wave height, as calculated from the pitch-and-roll buoy spectrum, was 1.8 m. The corresponding radar-derived frequency spectrum (Figure 3*b*) is obtained from the two-dimensional spectrum of the radar PPI image (Figures 4*a* and 4*b*) by integrating over the angles of a half plane and using the dispersion relation of surface waves for the actual water depth of 12.5 m in a similar manner as explained by *McLeish and Ross* [1983]. The spectrum derived from a radar image could only be determined in relative units. Therefore we have normalized the radar spectrum so that its peak height coincides with the peak height of the pitch-and-roll buoy spectrum. The method described in this paper resolves the directional ambiguity and produces a two-dimensional spectrum shown in Figure 4*c*. It

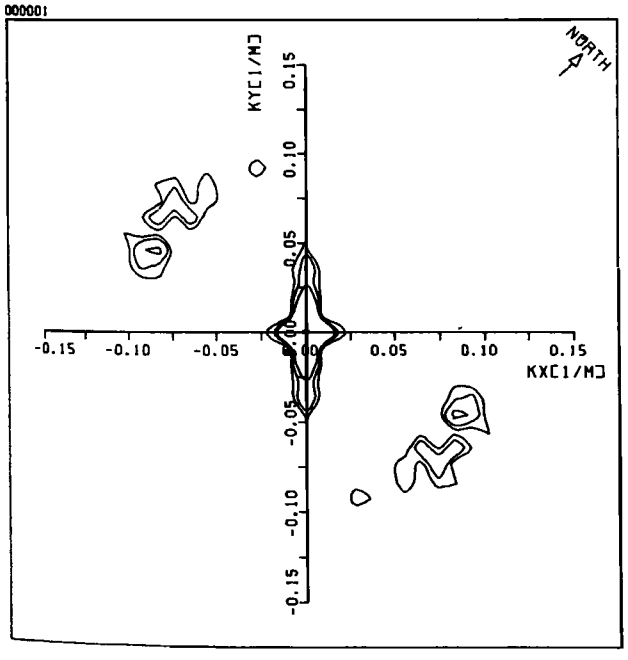

Fig. 4*b*

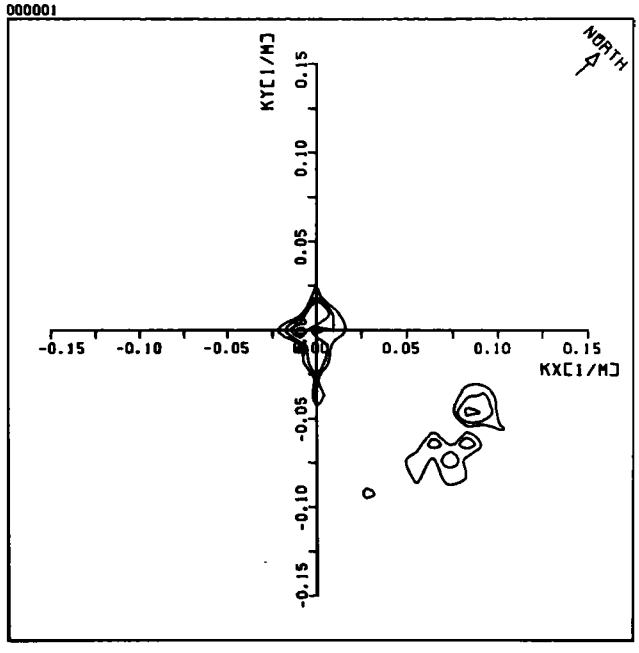

Fig. 4*c*

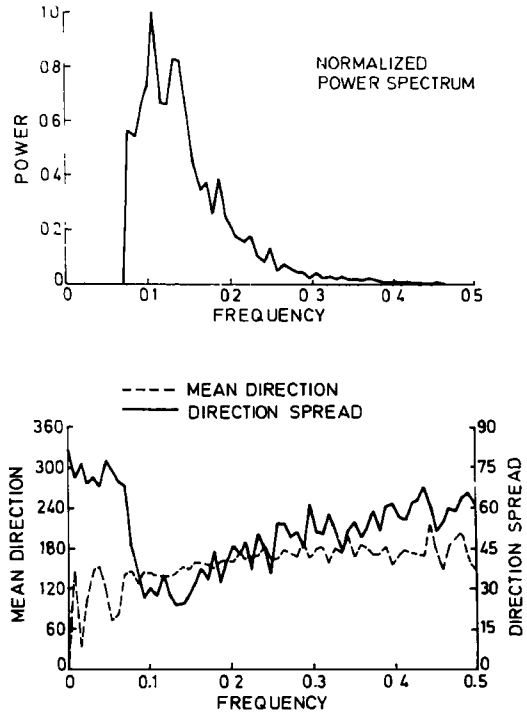

Fig. 5a

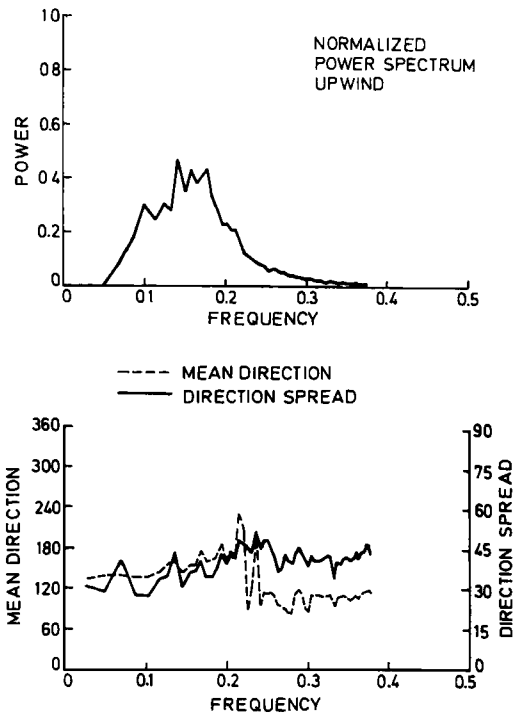

Fig. 5b

Fig. 5. (*a*) Pitch-and-roll buoy and (*b*) radar-obtained frequency spectra, mean direction, and angular spread in the case of combined sea and swell (case II).

is clear from Figure 4*c* that the waves are propagating toward the east. In future investigations it will be interesting to find out to what extent upwind traveling waves could be distinguished above the noise level.

The second case we consider is a very confused sea state created by incoming swell and temporary changing local wind, with a speed of 15.4 m/s, coming from 350°, with possible variability up to 20°. The significant wave height given by the pitch-and-roll buoy was 2.3 m. The ship was heading to 263° and drifting to 158° with velocity of 0.9 m/s over ground. The water depth was 30 m. The comparison of the one dimensional spectra derived from pitch-and-roll buoy and radar, depicted in Figure 5, is not as favorable as in the previous case. We normalized the radar spectrum such that the high-frequency tail of the radar spectrum has a similar height as that from pitch-and-roll buoy data. The low-frequency discrepancies

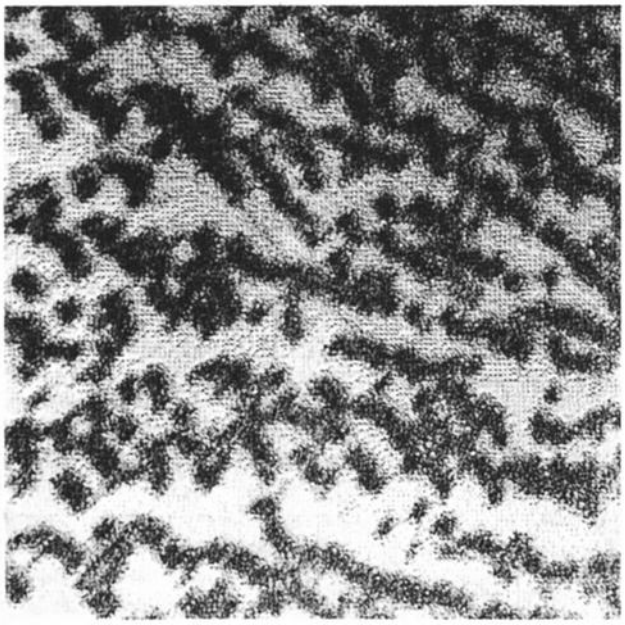

Fig. 6a

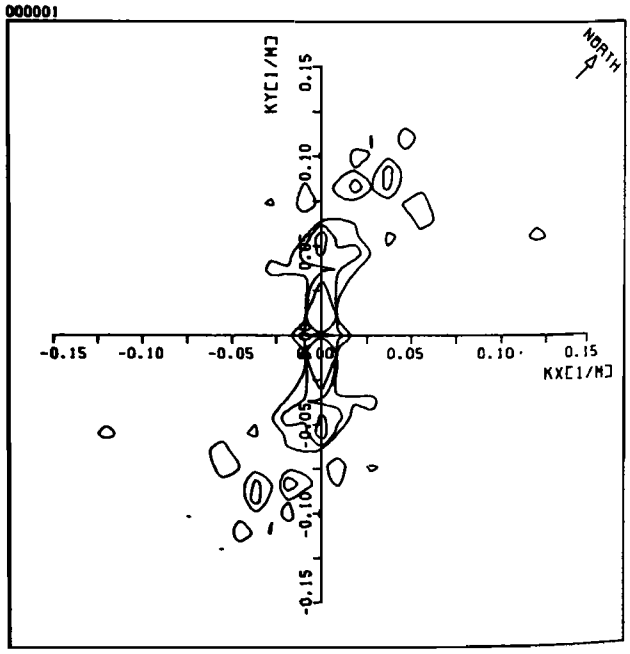

Fig. 6b

Fig. 6. (*a*) Gray scale radar PPI image and its two-dimensional power spectra (*b*) with and (*c*) without ambiguity in the case of sea and swell. The isolines are the same as in Figure 4.

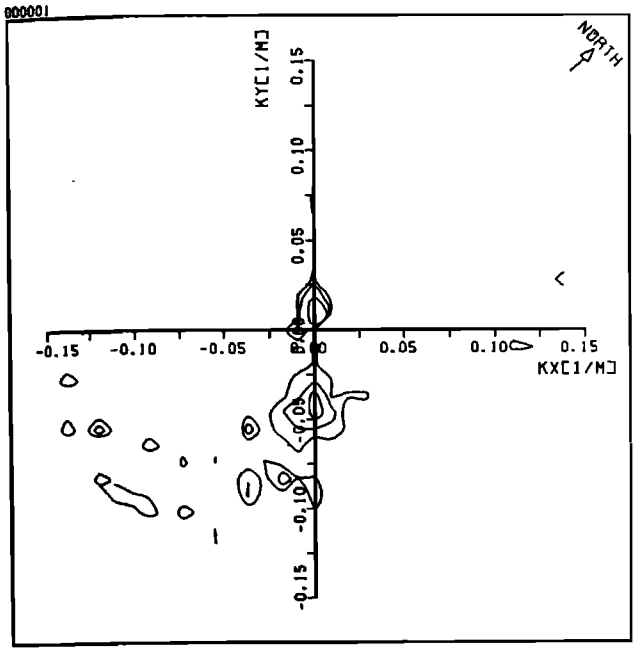

Fig. 6c

might be explainable by sampling variability, but a detailed investigation of those goes beyond the topic of this paper. The method proposed in section 2 is applied to the radar data. The difference between the conventional ambiguous two-dimensional spectrum and the unambiguous proposal can be seen in Figures 6*b* and 6*c*. Again the main propagation is resolved to be in downwind direction. Upwind traveling components can be observed in the spectrum. It is, however, not sure whether these are artifacts generated by errors in the assumed dispersion law due to incomplete knowledge of the ship drift or of the current velocity.

5. CONCLUSION

We have demonstrated the possibility of resolving the ambiguity of the two-dimensional surface wave spectra obtained by processing ship radar images. This ambiguity appears if the "frozen" surface at one specific time is used for the derivation of the power spectrum. By using two successive images it is possible to generate unique two-dimensional power spectra, which may be useful in many situations to determine the actual direction of wave propagation as well as, less evidently, to investigate wave reflection and upwind traveling waves. In addition, it may aid in choosing the correct wind direction from the multiple solution in algorithms for wind direction of satellite scatterometers, for instance SASS in Seasat. Instead of mixing four successive SAR images to reduce the speckle, they may be used to remove the wave propagation ambiguity. The wind direction should be approximately parallel to the shortest wind waves resolved by the imaging radar.

Acknowledgments. This work has been done within Sonderforschungsbereich 94 supported by Deutsche Forschungsgemeinschaft. The authors are indebted to K. Richter from Deutsches Hydrographisches Institut, who supported equipment and made ship time available. One of us (V.A.) is grateful to K. Hasselmann and J. Sündermann for their hospitality as well as to Deutscher Akademischer Austauschdienst for the financial support.

REFERENCES

Alpers, W. R., D. B. Ross, and C. L. Rufenach, On the detectability of ocean surface waves by real and synthetic aperture radar, *J. Geophys. Res.*, *86*, 6481–6498, 1981.

Braun, A., Critical analysis of DSA5 model and expected improvements, in *Wave and Wind Directionality, International Conference, Paris Sept. 29–Oct. 1, 1981, Collect. Colloq. Semin.*, vol. 36, pp. 143–149, Editions Technip, Paris, 1982.

Holthuijsen, L. H., Observation of the directional distribution of ocean-wave energy in fetch-limited conditions, *J. Phys. Oceanogr.*, *13*, 191–207, 1983.

Hoogeboom, P., and W. Rosenthal, Directional wave spectra images, paper presented at the International Geoscience and Remote Sensing Symposium, IEEE Geosci. and Remote Sensing Soc., Munich, June 1–4, 1982.

Long, R. B., Scattering of surface waves by an irregular bottom, *J. Geophys. Res.*, *78*, 7861–7870, 1973.

Mattie, M. G., and D. L. Harris, The use of imaging radar in studying ocean waves, paper presented at the 16th Coastal Engineering Conference, Am. Soc. of Civ. Eng., Hamburg, Aug. 28–Sept. 1, 1978.

Mattie, M. G., V. S. Hsiao, and D. D. Evans, Wave direction measured by four different systems, *IEEE J. Oceanic Eng.*, *OE-6*, 87–93, 1981.

McLeish, W., and D. B. Ross, Imaging radar observations of directional properties of ocean waves, *J. Geophys. Res.*, *88*, 4407–4419, 1983.

McLeish, W., D. Ross, R. A. Shuchman, P. Teleki, S. V. Hsiao, O. H. Shemdin, and W. E. Brown, Synthetic aperture radar imaging of ocean waves: Comparison with wave measurements, *J. Geophys. Res.*, *85*, 5003–5011, 1980.

Wadhams, P., Wave decay in the marginal ice zone measured from a submarine, *Deep Sea Res.*, *25*, 23–40, 1978.

Ziemer, F., and W. Rosenthal, Measurements of the directional wave spectra by ship radar, paper presented at the IAPSO Symposium PS-11, IUGG XVIII General Assembly, Hamburg, 1983.

V. Atanassov, W. Rosenthal, and F. Ziemer, Max-Planck-Institut für Meteorologie, Bundestrasse 55-Geomatikum, D-2000 Hamburg 13, Federal Republic of Germany.

(Received December 21, 1983;
accepted June 21, 1984.)